JMEPEG
https://doi.org/10.1007/s11665-023-08555-4

1059-9495/$19.00

ORIGINAL RESEARCH ARTICLE

Prediction of Cutting Forces in Hard Turning Process Using Machine Learning Methods: A Case Study

Souâd Makhfi, Abdelhakim Dorbane, Fouzi Harrou, and Ying Sun

Submitted: 24 March 2023 / Revised: 17 May 2023 / Accepted: 14 July 2023

Accurately predicting cutting forces in hard turning processes can lead to improved process control, reduced tool wear, and enhanced productivity. This study aims to predict machining force components during the hard turning of AISI 52100 bearing steel using machine learning models. Specifically, eight models were considered, and their prediction performance was assessed using experimental data collected during AISI 52100 bearing steel turning with a CBN cutting tool. The fivefold cross-validation technique has been adopted in training to obtain more reliable estimates of the performance of a model and reduce the risk of overfitting the data. Results showed that the Gaussian process regression (GPR) and decision tree regression outperformed the other models, with averaged root-mean-square error values of 14.44 and 12.72, respectively. GPR also provided prediction uncertainty. Additionally, feature selection was performed using two algorithms, namely Regressional Relief-F and F test, to identify the most important features impacting the cutting forces. The findings of this study can be useful in optimizing cutting parameters for hard turning processes to select cutting forces, reduce tool wear, and minimize the generated heat during the machining process.

Keywords cutting force, hard turning operation, machine learning, prediction, variable importance

1. Introduction

Machining is a critical process in manufacturing, where specialized tools are used to remove material from a workpiece to achieve desired specifications. The success of this operation relies on factors such as cutting parameters, tool material, speed, and feed rate (Ref 1). Hard machining is an essential process that efficiently machines hardened steel parts, producing high-quality parts with high-dimensional accuracy and surface finish quality. It is beneficial in the manufacturing industry, where there is a growing demand for parts with high hardness and wear resistance. Furthermore, hard machining reduces lead time and manufacturing costs by eliminating the need for additional processes like heat treatment. However, without lubrication, hard machining exhibits unique characteristics like segmented chip formation and microstructural alterations at the machined surfaces that differ from conventional machining. The hard machining process's high cutting forces and temperatures affect various cutting process parameters, including dynamic stability, tool wear, workpiece surface integrity, geometrical tolerances, and times (Ref 2-5).

Over the last decades, various studies investigated the effects of various machining parameters on the hard turning of different steel workpieces. Branco et al. concluded that hard turning using cubic boron nitride (CBN) tools can replace the grinding process, resulting in reduced machining time and costs (Ref 6). Kumar et al. found that cutting forces and surface roughness are affected by the alloying elements and percentage of CBN in the cutting tool material, while work material hardness, feed rate, and cutting speed are statistically significant in the responses (Ref 7). Azizi et al. optimized machining parameters in hard turning of EN19 alloy steel under dry conditions with coated carbide cutting tools using RSM mathematical models, which were confirmed by the experiments (Ref 3). Moreover, Umamaheswarrao et al. investigated the impact of cutting parameters and tool geometry on machining forces in hard turning of AISI 52100 in dry conditions with polycrystalline cubic boron nitride (PCBN) tool using surface defect machining (SDM) method (Ref 8). Results showed that surface defect hard turning reduced average machining force by 22% compared to conventional hard turning. Cappellini and Abeni proposed a new analytical model of tool wear for hard turning of AISI 52100 using PCBN inserts (Ref 9). They used simulations to predict the progression of wear and study its impact on the process and validated the model by comparing the experimental and simulated wear parameters. Results showed good agreement between the two.

In recent years, the mechanical and production industries have faced challenges related to sustainable manufacturing (Ref 10-14). Machine learning has recently been increasingly used in material science and mechanical engineering to analyze large datasets, optimize designs, and predict material properties and system performance. It can be used to predict material

Souâd Makhfi, Research Laboratory of Industrial Technologies, Faculty of Applied Sciences, University of Tiaret, PO BOX 78, Zaâroura, 14000 Tiaret, Algeria; **Abdelhakim Dorbane**, Smart Structures Laboratory (SSL), Department of Mechanical Engineering, Faculty of Science and Technology, University of Ain Temouchent, PO BOX 284, 46000 Ain Temouchent, Algeria; and **Fouzi Harrou** and **Ying Sun**, Computer, Electrical and Mathematical Sciences and Engineering (CEMSE) Division, King Abdullah University of Science and Technology (KAUST), 23955-6900 Thuwal, Saudi Arabia. Contact e-mail: abdelhakim.dorbane@univ-temouchent.edu.dz.

Published online: 07 August 2023

properties and behavior (Ref 15) and identify new materials for specific applications (Ref 16, 17), as well as optimize designs and predict the performance of mechanical systems (Ref 18). Machine learning can also identify and diagnose faults and failures in mechanical systems, leading to cost savings and improved performance and reliability (Ref 19). Its application in material science and mechanical engineering can accelerate research and development, reduce costs, and improve the performance and reliability of mechanical systems and materials.

Machine learning has emerged as a useful tool for predicting output parameters that determine the quality of final products in hard turning processes (Ref 20). In (Ref 21), Cica et al. applied three regression-based machine learning techniques, namely support vector regression (SVR), Gaussian process regression (GPR), and polynomial regression (PR), to predict cutting power, cutting pressure, and machining force in the hard turning of AISI 1045 employing tool carbide tools. They considered control factors such as cutting speed, depth of cut, and feed rate while using minimum lubricant quantity and high-pressure coolant-assisted turning. Results show that both SVR and GPR models achieved satisfactory predictions and outperformed the PR model. Das et al. compared the effectiveness of polynomial regression (PR), random forest (RF) regression, gradient boosted (GB) trees, and adaptive boosting (AB)-based regression to predict machining outputs such as surface roughness and cutting force (Ref 22). They concluded that PR was the best model for their study of machining AISI D6 steel with an AlTiSiN-coated carbide tool in dry-cutting conditions. The authors also identified the optimal machining parameters to minimize output parameters as speed (60 m/min), feed rate (0.04 mm/rev), and depth of cut (0.2 mm). In (Ref 23), Du et al. investigated a machine learning technique to predict surface roughness, profile, and roundness in hard turning. The authors used sensor signals as inputs and evaluated model accuracy by comparing predicted and measured data. The proposed ML model showed promising results, with $R2$ values of 0.92 for roughness, 0.86 for profile deviation, and 0.95 for roundness deviation. This study concluded that the frequency-domain feature extraction technique developed effectively extracted relevant features from signals. Makhfi et al. (Ref 24) presented an ANN model to predict cutting force components during hard turning of AISI 52100 bearing steel using CBN cutting tools. The ANN model used cutting speed, feed rate, depth of cut, and workpiece hardness as input parameters and the three cutting force components as output data. A feed-forward single hidden layer ANN trained by BR/LM achieved the best prediction accuracy, with an average error of 11.47% on Fa and Fr and 6.17% on Ft, using an 11-neuron hidden layer and sigmoid activation function on the hidden layer and linear on the output layer. This study (Ref 25) investigated the machinability of AISI 52100 bearing steel during finish turning. A coated carbide with a multilayer insert performed best in wear and surface quality. Machining variables were modeled through quadratic regression and artificial neural networks. Multi-parametric optimization was achieved through Taguchi-based grey relational analysis, resulting in an optimal parametric combination. The ANN model yields more accurate response predictions in this study. The tool life at optimized cutting conditions was approximately 19 minutes. This study (Ref 26) compared RSM and ANN models in predicting surface roughness in machining AISI 1040 steel. ANN performed slightly better. The optimal parameters for the lowest roughness were a depth of cut of 0.1 mm, feed of 0.04 mm/rev, and cutting speed of 260 m/min. Kumar et al. (Ref 27) studied the use of mixed ceramic inserts in hard turning with accelerated cooling to prevent tool tip fracture. The optimal parameter combination was d1-f1-v2 (0.1mm-0.04 m/min-108 m/min), resulting in improved machinability, tool life, and reduced machining cost, with satisfactory flank wear and surface roughness. Panda et al. (Ref 28) optimized surface quality in hard turning of EN31 steel using a multilayer coated carbide insert. They used Taguchi's L9 orthogonal array and linear regression analysis to identify significant cutting parameters affecting surface quality, which were feed and depth of cut. Sahoo et al. (Ref 29) investigated multilayer coated carbide inserts in hard turning of AISI 4340 steel to evaluate tool life and wear. They found abrasion to be the dominant wear mechanism, with a tool life of 31 minutes. Their mathematical model had a high determination coefficient and accurately predicted flank wear at a 95% confidence level. In (Ref 30), Das et al. compared the machinability of heat-treated 4340 steel in dry and minimum quantity lubrication (MQL) environments using multilayer coated carbide inserts. Abrasion was the primary wear mechanism under both conditions, with cutting speed being the most important process parameter. The study found that the inserts performed better in the MQL condition, resulting in a higher surface finish than in the dry condition.

While previous studies have investigated the use of machine learning methods for predicting machining forces in other materials or machining processes, the focus of this study is to develop and compare machine learning models for predicting the three cutting force components during hard turning of AISI 52100 bearing steel, which is an important material used in various industrial applications (Ref 31). AISI 52100 is widely used for manufacturing hardened parts with tight tolerances, longer service life, and a good surface finish (Ref 5, 8, 32). Predicting machining force components is crucial in the hard turning of AISI 52100 bearing steel. It helps select cutting parameters, detect problems during the process, and maintain process stability, modeling, and simulation. Accurate prediction of machining forces improves productivity, surface quality, and tool life while reducing the risk of tool breakage and damage to the workpiece (Ref 24). This study considered eight machine learning models, including linear regression (LR), principal component regression (PCR), partial least square regression (PLSR), support vector regression (SVR), decision tree regression (DTR), ensemble learning-based regression, NN, and Gaussian GPR. The fivefold cross-validation technique has been adopted in training to obtain more reliable estimates of the performance of a model and reduce the risk of overfitting the data. Experimental data collected during AISI 52100 bearing steel turning with a CBN cutting tool were used to assess the models' prediction performance. Results showed that the GPR and DT regression outperformed the other models. The results demonstrate GPR's ability to predict machining forces and provide prediction uncertainty. The study also performed feature selection using Regressional Relief-F (RReliefF) and F test algorithms to identify the most important features affecting cutting forces. This information can be useful in optimizing the cutting parameters for hard turning processes to minimize cutting forces and reduce tool wear.

2. Material and Methods

2.1 Data Description and Analysis

The experiments were carried out on a CNC lathe-type Ramo (RACN82) in turning operation out in dry condition by CBN inserts ISO VBGW160408NC2 BNX 10 by Sumitomo Company. The cutting process involves the rotation of the workpiece, while the cutting tool has a feed rate. The cutting force components are measured using a piezoelectric dynamometer Kistler. The experiments were conducted under dry conditions, meaning no cutting fluid or coolant was used during the cutting process.

Workpiece material: The workpiece was made of AISI 52100 bearing steel, a common material in the industry due to its high strength, hardness, and wear resistance (Ref 5, 8, 32). The material had a hardness range of 45 to 55.25 HRC after heat treatment and was in a tube shape with a diameter of 88 mm, thickness of 10 to 30 mm, and a length of 110 mm. The workpiece dimensions presented challenges in the machining process. The chemical composition of the work material is reported in Table 1 (Ref 15). The cutting parameters ranged as follows: workpiece hardness: HRC = [45 to 55.25] with five levels; cutting speed: Vc = [50 to 300] m/min with five levels; feed: f = [0.05 to 0.2] mm/rev with five levels; and depth of cut: ap = [0.1 to 0.4] mm with five levels. The AISI 52100 bearing steel is widely used in various applications, including manufacturing hardened parts that require tight geometric tolerances, longer service life, and a good surface finish (Ref 2).

Tool material: The main tool materials used in hard machining are CBN due to their high hardness and, in the case of some grades of these materials, high chemical stability with iron. The CBN tools showed much better performance with respect tool life and part surface roughness (Ref 33, 21, 8). However, CBN tool generates high temperature and force during cutting in hard turning. To overcome these problems, cutting tool is provided with negative rake angle, but if this rake angles value is increased, then it gives rise to high compressive stress (Ref 34). The cutting tool geometry plays a very significant role in hard turning process (Ref 7, 9). In this study, CBN inserts with BNX 10 grade by negative chamfered edge (20° × 0.1 mm) are used. The physical characteristics of the insert are given in Table 2 (Ref 35).

Data collection: The objective of the experimental work was to investigate the influence of workpiece hardness (HRC) and cutting parameters (V_c, f, and a_p) on machining force components (F_f, F_r, and F_t) in hard turning of AISI 52100 bearing steel using CBN cutting tool. The components of machining force were measured by a piezoelectric dynamometer Kistler-type 9257B. Understanding how these factors affect machining force components can help improve the efficiency and quality of hard turning processes.

Figure 1 shows the machining force components (F_f, F_r, and F_t) during the hard turning of AISI 52100 steel using a CBN cutting tool.

Figure 1 demonstrates that the cutting forces (F_f and F_t) are relatively higher compared to the feed force (F_r) during the machining process. This is expected in hard turning as cutting forces are primarily responsible for material removal, while feed forces are responsible for moving the tool along the workpiece. Additionally, from Fig. 2, we observe the presence of a transient regime corresponding to the penetration of the cutting tool in the material, and then, the forces reach a stationary regime with the presence of a weak fluctuation around their average values considered as being the measured values of the components of the machining force. It is these values that are taken into account in the readings.

The experimental dataset is divided into two data-bases as training and test bases. On a total of 35 examples, 25 examples are intended for the training and 10 examples are used for the test which are given in Table 3 (Ref 2).

2.2 Machine Learning-Based Cutting Forces Prediction in Hard Turning Processes

This study investigates eight models: linear regression, principal component regression (PCR), partial least square regression (PLSR), decision tree regression (DTR), support vector regression, Gaussian process regression (GPR), neural network, and ensemble learning-based regression. Next, we describe briefly these approaches.

(1) Linear regression (LR): Linear regression is a traditional statistical method used to model the linear relationship between the input and output variables. The model is represented as a simple equation.

$$y = \beta_0 + \beta_1 x_1 + \beta_2 x_2 + \ldots + \beta_n \times x_n + \varepsilon \qquad \text{(Eq 1)}$$

where y is the output variable, x_1, x_2, ..., x_n are the input variables, β_0, β_1, β_2, ..., βn are the model parameters or coefficients, and ε is the error term. The LR model assumes that the relationship between the variables is linear, meaning that a change in one variable is proportional to a change in the other variables. LR regression works by finding the line of best fit that minimizes the sum of the squared differences between the predicted values and the actual values of the dependent variable. However, it has some limitations, such as the assumption of linearity and the possibility of overfitting if the model is too complex or the sample size is too small.

(2) Principal component regression (PCR): PCR is a method that combines principal component analysis (PCA) and linear regression to handle multicollinearity in the input data (Ref 36). The basic idea is to reduce the dimensionality of the input data by projecting it onto a lower-dimensional space using PCA and then use linear regression to model the relationship between the reduced input variables and the output variable (Ref 37). The model can be expressed as:

Table 1 Chemical composition (%) of AISI 52100

Element	% C	% Cr	% Cu	% S	% Si	% Mo	% Mn	% P
Measured value	1.05	1.481	0.033	0.018	0.239	0.01	0.365	0.009

$$y = \beta_0 + \beta_1 z_1 + \beta_2 z_2 + \ldots + \beta_k \times z_k + \varepsilon \quad \text{(Eq 2)}$$

where y is the output variable, z_1, z_2, ..., z_k are the k principal components obtained from PCA, β_0, β_1, β_2, ..., β_k are the model parameters, and ε is the error term.

(3) Partial least square regression: PLSR is a regression method that combines principal component analysis (PCA) and linear regression to predict a response variable from many highly correlated predictor variables. PLSR creates a new set of variables, called latent variables or components, that are linear combinations of the original predictor variables, and then uses these latent variables as predictors in a linear regression model (Ref 38). PLSR is expressed mathematically using X, an $n \times p$ matrix of predictor variables, where n is the number of observations and p is the number of original predictor variables, and Y, an $n \times 1$ vector of response variable values. PLSR first creates a set of k latent variables, denoted by T_1, T_2, ..., T_k, and U_1, U_2, ..., U_k, where k is typically chosen to be less than or equal to the number of original predictor variables. The first latent variable T_1 is defined as a linear combination of the original predictor variables X_1, X_2, ..., X_p:

$$T_1 = X_1 w_{11} + X_2 w_{21} + \ldots + X_p \times w_{p1} \quad \text{(Eq 3)}$$

where w_{11}, w_{21}, ..., w_{p1} are the weights or loadings for the first latent variable. The weights are chosen to maximize the covariance between T_1 and Y, subject to the constraint that the weights have unit length. Similarly, the first score vector U_1 is defined as a linear combination of the response variable Y: $U_1 = Y \times c_{11}$, where c_{11} is a scalar that scales U_1 to have unit length. The subsequent latent variables T_2, T_3, ..., T_k and U_2, U_3, ..., U_k are obtained in a similar manner, but with the constraint that they are orthogonal (uncorrelated) to the previous latent variables.

Once the latent variables are obtained, PLSR uses them as predictors in a linear regression model to predict the response variable Y:

$$Y = b_0 + b_1 T_1 + b_2 T_2 + \ldots + b_k \times T_k + e, \quad \text{(Eq 4)}$$

where b_0, b_1, b_2, ..., b_k are the regression coefficients, and e is the error term. PLSR can be used for both prediction and variable selection. The number of latent variables to use in the model can be chosen using techniques such as cross-validation or the explained variance criterion. By using only a subset of the latent variables, we can perform variable selection and eliminate unimportant predictor variables.

(4) Decision tree regression: DTR is a machine learning algorithm that creates a tree-like model of decisions and their possible outcomes based on input features and output values (Ref 39). It partitions the training dataset recursively into smaller subsets based on the value of a chosen input feature, where each partition is defined by a decision rule or splitting criterion that maximizes the homogeneity of the output values within the subset. The output is a tree-like model of decisions, where each node represents a decision rule, and each leaf represents a predicted output value. DTR has the advantage of handling nonlinear relationships between input and output variables and being easily interpretable. However, it is prone to overfitting and may require pruning or regularization to improve generalization performance.

(5) Support vector regression: SVR is a flexible data-based approach that leverages kernel techniques to achieve effective learning. The fundamental concept behind SVR involves mapping the training data to a higher-dimensional space and then performing linear regression. Notably, SVR can handle nonlinear and non-separable

Table 2 Physical characteristics of the insert

Sumitomo shade	Coating	Hardness, GPa	Thermal conductivity, W/mK	TRS, GPa
BNX 10	Without	27-31	40	800-900

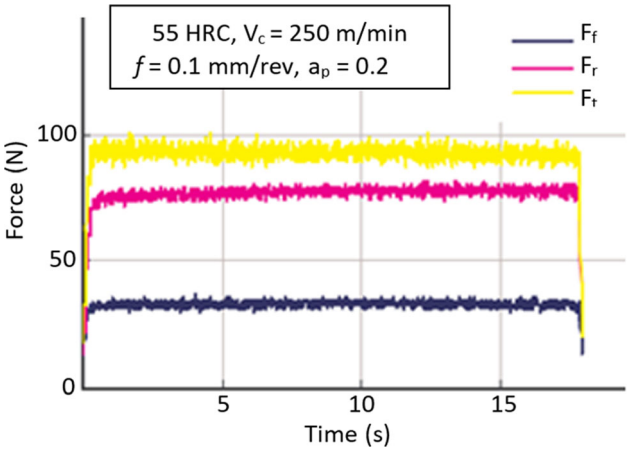

Fig. 1 Machining force components during turning of AISI 5200 steel

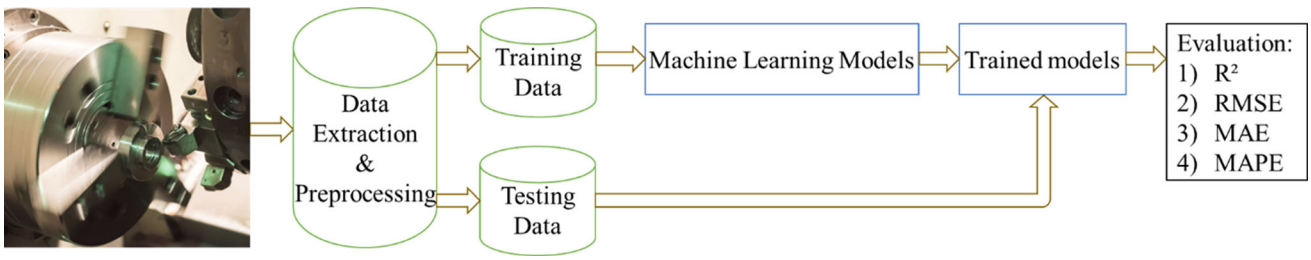

Fig. 2 Flowchart of proposed framework for predicting using machine learning

Table 3 Summary of eight regression models used in the study, including their pros and cons

Model	Approach	Pros	Cons	Concept
Linear regression	Linear relationship between input features and output target	Simple, easy to interpret, fast computation	Assumes linearity, sensitive to outliers	Regression, linearity
PCR	Combination of PCA and linear regression	Improves multicollinearity, reduces noise	May lead to overfitting, requires determination of components	Dimension reduction, regression
PLSR	Combination of PCA and linear regression	Handles multicollinearity, reduces noise, improves prediction	May lead to overfitting, requires determination of components	Dimension reduction, regression
DTR	Decision tree algorithm	Nonlinear relationships, handles categorical features	Prone to overfitting, may generate complex trees	Nonlinearity, decision trees
Support vector regression	Mapping input features to higher dimensions to find a hyperplane that best separates the output target from the input features	Handles nonlinear relationships, robust to outliers	Computationally expensive, requires tuning of kernel parameters	Nonlinearity, hyperplanes
GPR	Modeling the output target as a Gaussian process	Handles nonlinear relationships, provides uncertainty estimates	Computationally expensive, may not scale well with large datasets	Nonlinearity, Gaussian processes
Neural network	Combination of interconnected neurons	Handles nonlinear relationships, can model complex functions	Computationally expensive, may lead to overfitting	Nonlinearity, interconnected neurons, deep learning
Ensemble learning-based regression	Combination of multiple regression models	Robust to overfitting, improves prediction accuracy	Computationally expensive, may not scale well with large datasets	Regression, model combination

data through kernel tricks and can manage large feature datasets while being robust to outliers. However, the SVR model demands significant computational resources and may be sensitive to kernel function selection and regularization parameter selection (Ref 40). *Structural risk minimization* is the key concept underpinning the development of SVR. Prior studies have shown that SVR performs well with limited sample sizes (Ref 41), making it a popular choice in a wide range of applications, including solar irradiance, wind power prediction, and anomaly detection (Ref 42-44).

(6) Gaussian process regression: GPR is a probabilistic machine learning method used for regression and classification problems (Ref 45). It models the target variable as a Gaussian process, assigning a probability distribution to predicted values. GPR is nonparametric and can capture complex relationships between input and target variables (Ref 46). During training, the model learns the hyperparameters of the covariance function by maximizing the likelihood of the observed data. GPR can model uncertainty in predictions and is useful in critical applications like medical diagnoses or financial forecasting. It is flexible and can handle regression and classification tasks. However, it can be computationally expensive for large datasets and is sensitive to the choice of covariance function and hyperparameters.

(7) Neural network: Artificial neural networks (ANNs) are powerful models that could recognize complex relationships between inputs and outputs. A trilayered neural network is used in this study, which contains three layers: an input layer, a hidden layer, and an output layer, for a prediction task. The input layer receives data, which is then processed by the hidden layer using weights and biases. The output of the hidden layer is passed through an activation function, and the output layer produces the final prediction. Using a trilayered neural network with three hidden layers allows more complex relationships to be learned than simpler architectures. However, using a more complex model can increase the risk of overfitting, so regularization techniques like dropout or weight decay are important to use.

(8) Ensemble learning-based regression: Bagging decision trees is an ensemble learning technique that uses multiple decision trees to improve prediction accuracy and robustness (Ref 47). The method trains decision trees independently using different bootstrap samples from the original dataset, resulting in diverse trees. The bagging algorithm aggregates the decision trees' outputs to make predictions, taking the majority vote in classification and average in regression. Bagging reduces model variance, which helps to avoid overfitting and handle noisy and complex datasets. However, it may increase model bias if the trees are too simple or not enough trees are used.

2.3 The Proposed Framework

This section presents the machine learning-based forecasting framework adopted to prediction framework for the three cutting force components in hard turning processes. Figure 2 shows a schematic description of the proposed machine learning-based prediction framework. The framework consists of four main steps: data acquisition and preprocessing model training, and model evaluation. Data are acquired using sensors and stored in a database in the first step. The features are extracted from the acquired data, such as the cutting speed (V_c), feed (f), depth of cut (a_p), and the hardness of the workpiece material (HRC). These features are then preprocessed to remove any noise and outliers.

In the second step, we train the investigated machine learning models to predict the three components of cutting force. The model was trained using cross-validation, with the dataset being split into k-folds. The model was trained on k-1-folds for each fold and tested on the remaining fold. In k-fold cross-validation, the data are divided into k subsets or folds, and the model is trained and tested k times. Each iteration uses one fold as the test set and the remaining k-1-folds as the training set. The process is repeated until each fold has been used as the test set. The results were averaged across all folds to estimate the model's performance. Importantly, using cross-validation during the model training process helps to estimate the model's performance on an independent dataset and evaluate how well the model generalizes to new data. It also helps to avoid overfitting, which occurs when the model fits too closely to the training data and performs poorly on new data. In this study, fivefold cross-validation is adopted in training. The trained model is then validated using a testing dataset. In the final step, the model evaluation is conducted by comparing the predicted values with the actual values. The evaluation metrics used are the coefficient of determination (R^2), mean absolute error (MAE), root-mean-squared error (RMSE), and MAPE (mean absolute percentage error). R^2 represents the model's goodness of fit, where a value closer to 1 indicates a better fit. RMSE, MAE, and MAPE represent the accuracy of the model's predictions, where lower values indicate better performance.

- R^2 (Coefficient of determination): R^2 represents the proportion of variance in the target variable that is predictable from the independent variables.

$$R^2 = \frac{\sum_{t=1}^{n}[(y_t - \bar{y}) \cdot (\hat{y}_t - \bar{y})]^2}{\sqrt{\sum_{t=1}^{n}(y_t - \bar{y})^2} \cdot \sqrt{\sum_{t=1}^{n}(\hat{y}_t - \bar{y})^2}} \quad \text{(Eq 5)}$$

- RMSE (Root-mean-square error): RMSE measures the difference between the predicted and actual values in terms of the standard deviation of the error

$$\text{RMSE} = \sqrt{\frac{1}{n}\sum_{t=1}^{n}(y_t - \hat{y}_t)^2} \quad \text{(Eq 6)}$$

- MAE (Mean absolute error): MAE measures the absolute difference between the predicted and actual values.

$$\text{MAE} = \frac{\sum_{t=1}^{n}|y_t - \hat{y}_t|}{n} \quad \text{(Eq 7)}$$

- MAPE (Mean absolute percentage error): MAPE measures the percentage difference between the predicted and actual values.

$$\text{MAPE} = \frac{100}{n}\sum_{t=1}^{n}\left|\frac{y_t - \hat{y}_t}{y_t}\right|\% \quad \text{(Eq 8)}$$

where n is the number of samples, y is the actual value of the response variable for the ith sample, and $\hat{y}_i$ is the predicted value for the ith sample.

3. Results and Discussion

3.1 Statistical Data Analysis

In Fig. 3, we can see the distribution of the collected data, which shows that the variables HRC, Ff, and Fr are non-Gaussian distributed. This poses a challenge for traditional machine learning methods such as linear regression, principal component regression, and partial least square regression, which are designed based on the assumption that the input data follow a Gaussian distribution. Non-Gaussian data can lead to biased and unreliable results when using these traditional methods. However, there are other machine learning algorithms that can handle non-Gaussian data, such as decision tree regression, support vector regression, Gaussian process regression, and neural network regression. These algorithms do not rely on the Gaussian assumption and can be effective in predicting the machining force components in hard turning processes.

Figure 4 depicts the pairwise correlation coefficients between cutting parameters and machining force components during the hard turning of AISI 52100 bearing steel using a CBN cutting tool. We observe statistically significant relationships between the depth of cut (a_p) and each of the three components of the cutting force (F_f, F_r, and F_t). Specifically, the correlation coefficient of 0.7049 between the depth of cut (a_p) and the feed (f) suggests a moderate positive correlation between these two factors. This means that as the depth of cut increases, the feed also tends to increase. This is likely because deeper cuts require more material to be removed, which requires a higher feed to maintain a consistent cutting speed and avoid excessive tool wear or failure. The correlation coefficient of 0.4949 between the depth of depth (a_p) and the tangential force (F_t) suggests a moderate positive correlation between these two factors. This means that as the depth of cut increases, the tangential force (which is in the direction of cutting) also tends to increase. This is likely because deeper cuts require more material to be removed, which in turn requires a higher tangential force to overcome the resistance of the workpiece material. We observe a weak positive correlation of 0.3203 between the depth of cut (a_p) and the radial force (F_r). This means that as the depth of cut increases, the radial force (which is perpendicular to the direction of cutting) tends to increase slightly as well. This could be due to a number of factors, such as increased cutting-edge engagement or changes in chip formation as the depth of cut increases. Figure 4 shows strong

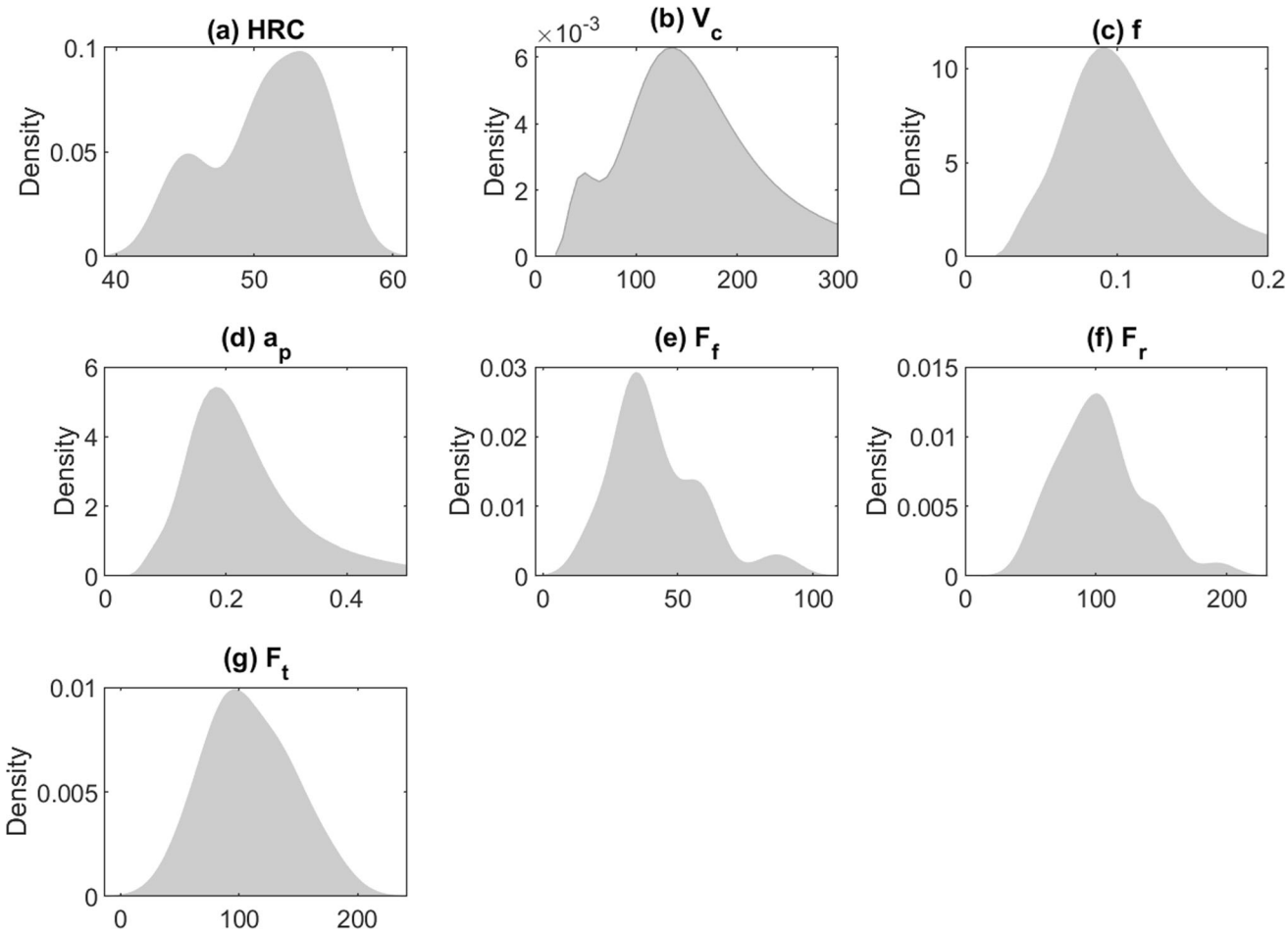

Fig. 3 Distribution of the considered data

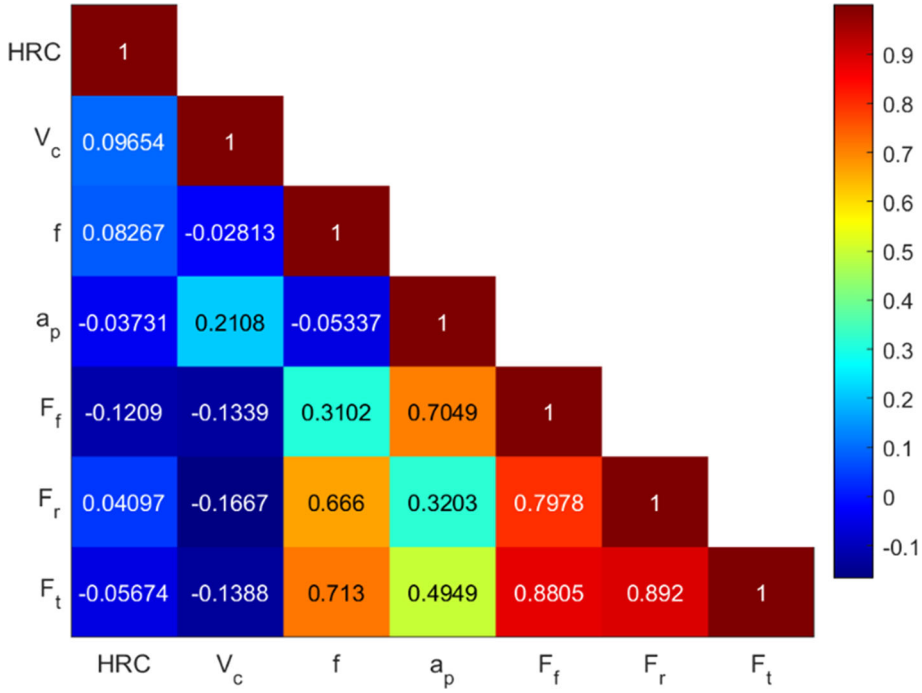

Fig. 4 Correlation matrix of the data

positive relationships between the three components of machining force (F_f, F_r, and F_t) during hard turning. Specifically, the tangential force (F_t) and the feed force (F_f) are positively correlated with a correlation coefficient of 0.8805. This could be due to factors such as increased tool engagement or changes in chip formation. Similarly, the correlation coefficient of 0.892 between the tangential force (F_t) and the radial force (F_r) also suggests a strong positive correlation between these two components of force. This could be due to changes in chip formation or increased tool wear. Finally, there is a high correlation of 0.7978 between the feed force (F_f) and the radial force (F_r). Of course, these correlations indicate that the three components of machining force (F_f, F_r, and F_t) are closely related and tend to increase or decrease together during hard turning.

Overall, these correlations provide valuable insights into the relationships between cutting parameters and machining force components. By understanding these relationships, engineers and manufacturers can make more informed decisions about selecting and optimizing cutting parameters to achieve optimal machining efficiency and tool life.

Figure 5 shows the empirical ACF of data. From the empirical ACF (autocorrelation function) of the data, it appears that the HRC variable is highly autocorrelated, meaning that it is strongly correlated with its past values. On the other hand, the other variables (V_c, f, and a_p) are weakly autocorrelated, indicating that they are not strongly dependent on their past values.

3.2 Prediction Results

This experimental study divided the dataset into two parts: a training set and a test set. The total dataset contained 35 examples, out of which 25 examples were used for training the models, and the remaining ten were kept for testing the models. The purpose of dividing the dataset into training and test sets is to train the models on a subset of the data and evaluate their performance on a different subset of the data that the models have not seen before. This helps to assess the generalization ability of the models and ensure that they can make accurate predictions on new, unseen data.

(a) Feed force prediction

In the first experiment, the performance of eight models was evaluated for the prediction of Feed force. The models were trained using the training data, and their predictive performance was evaluated using unseen testing data. The prediction results of the feed force based on testing data are displayed in Fig. 6. In the figure, the points are connected by straight lines by default when plotting a set of points using the plot function. These lines are not the result of any calculation or intermediate values measured, but rather they are simply added for visualization purposes. The purpose of connecting the points with lines is to give a sense of continuity to the data and to help visualize any trends or patterns in the data. We observe that all models can track the trend of the feed force (Fig. 6). However, some models perform better than others in terms of accuracy. Visually, it is observed that the predictions made by SVR and NN are relatively far from the testing feed force data compared to the other models. This indicates that these models might not be suitable for accurate prediction of feed force in the hard turning process. It is important to note that evaluating the models' performance based on only visual comparison is insufficient.

The boxplots of the prediction errors (Fig. 7) provide a visual representation of the accuracy of each model in predicting the feed force. The boxplot summarizes the distribution of the prediction errors for each model, including the median, interquartile range (IQR), and range of the data. The boxplots show that the linear regression model has the largest prediction errors compared to the other models, indicating that

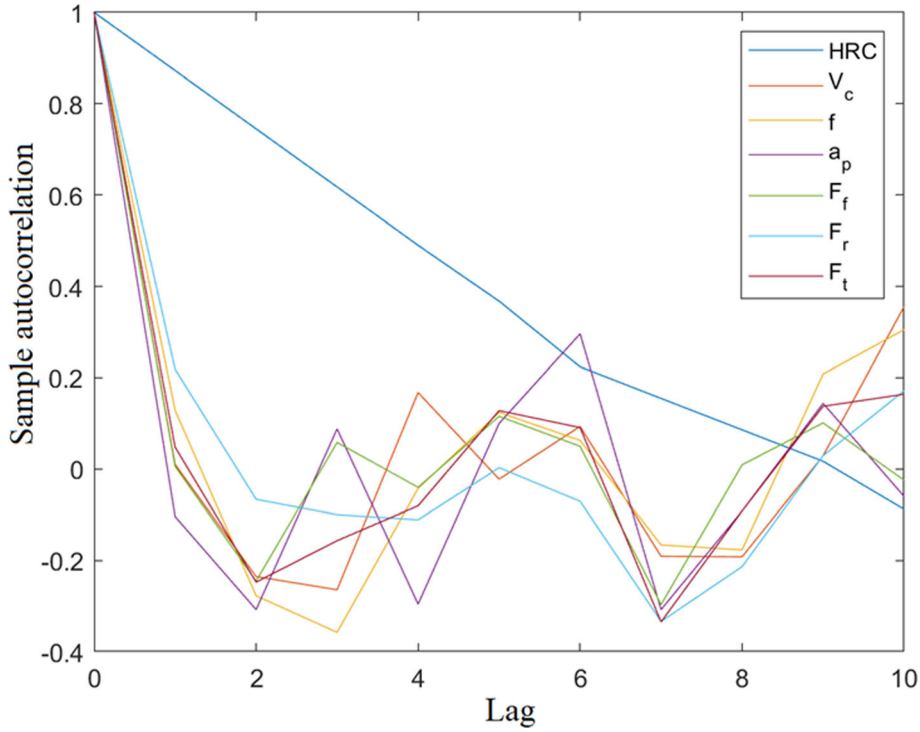

Fig. 5 ACF of the data

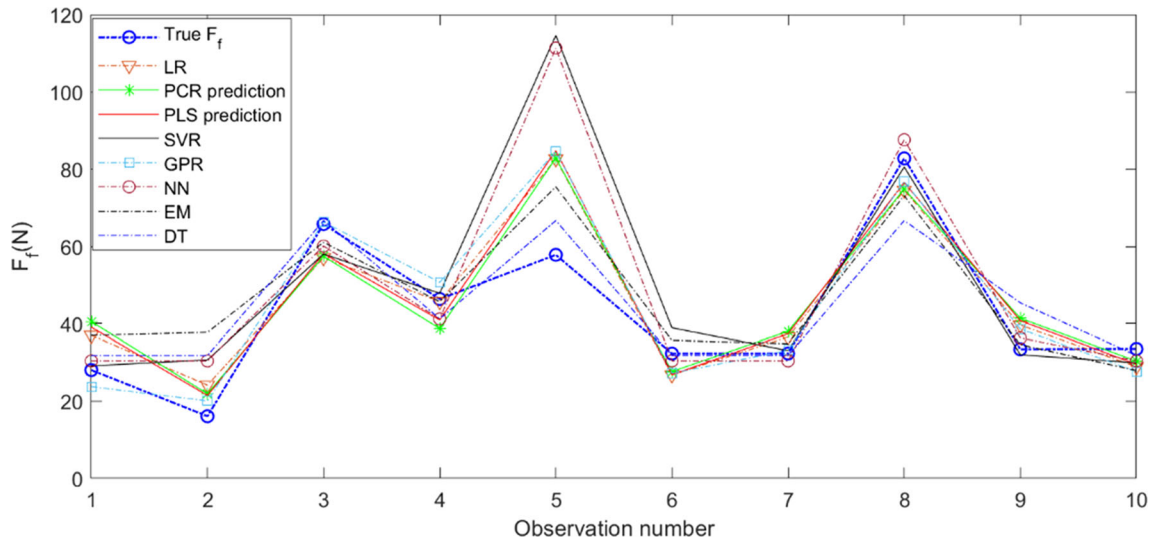

Fig. 6 Measured vs. predicted feed force using the eight models based on testing data

it is the least accurate in predicting the feed force. The ensemble learning-based regression and DTR models have the smallest prediction errors, indicating that they are the most accurate in predicting the feed force. The PLSR, PCR, and GPR models have relatively small prediction errors, indicating moderate accuracy. The SVR and NN models have the largest prediction errors, indicating that they are less accurate in predicting the feed force compared to the other models. Overall, the boxplots of the prediction errors provide valuable insights into the performance of each model and can assist in selecting the best model for predicting the feed force in hard turning.

Based on Table 4, the decision tree (DT) model has the lowest RMSE (8.79) and MAE (6.52) values, indicating the best accuracy among all the models. The DT model also has the highest R^2 value (0.80), indicating the best goodness of fit to the actual data. The Gaussian process regression (GPR) model has the lowest MAPE value (14.30%), indicating the lowest prediction error rate among all models. The linear regression (LR), partial least square regression (PLSR), and principal component regression (PCR) models have relatively similar performance, with RMSE and MAE values ranging between 10 and 11 and R^2 values around 0.70. The support vector regression (SVR) and neural network (NN) models have higher RMSE and MAE values and lower R^2 values, indicating lower

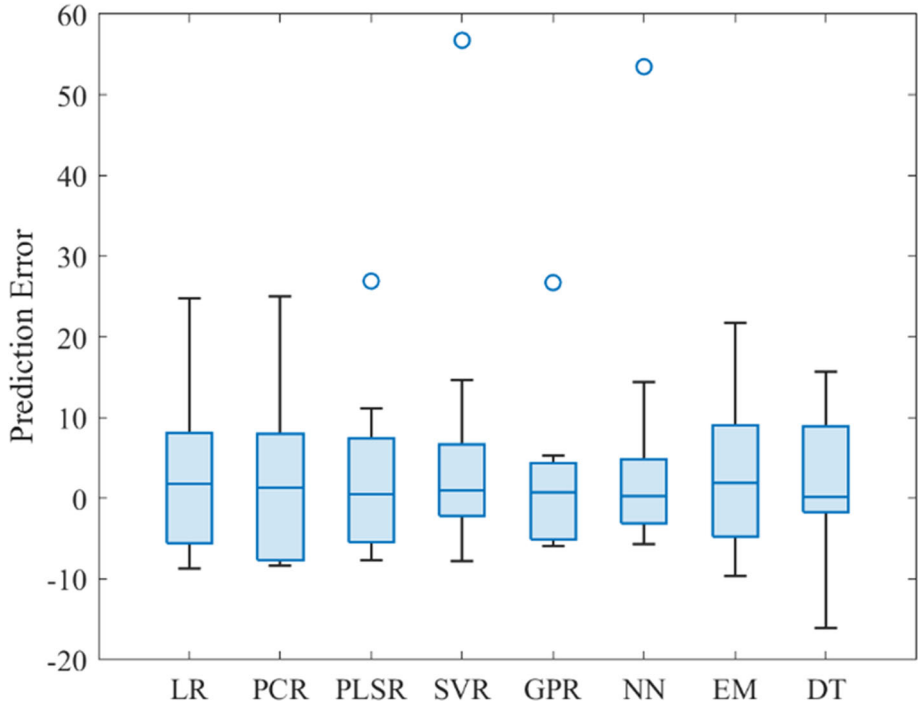

Fig. 7 Boxplots of prediction errors of the investigated models based on testing data

Table 4 Evaluation metrics over the testing sets for the eight models when predicting feed force

Method	RMSE	MAE	R^2	MAPE
LR	10.07	8.01	0.74	17.96
PCR	10.65	8.89	0.71	19.44
PLSR	10.63	8.47	0.71	18.56
SVR	18.87	9.63	0.16	15.59
GPR	9.45	6.29	0.77	14.30
NN	17.82	9.57	0.24	16.14
EM	10.13	7.60	0.75	16.76
DT	8.79	6.52	0.80	14.76

accuracy compared to the other models. Finally, the ensemble learning-based regression (EM) model has similar performance to the LR, PLSR, and PCR models, with slightly better accuracy than LR in terms of RMSE and MAE values and slightly worse in terms of R^2 value.

Also, based on Table 4, it can be seen that decision tree regression (DT) and Gaussian process regression (GPR) performed better than the other models in terms of RMSE, MAE, R^2, and MAPE. DT has the lowest RMSE and MAE values, indicating that it has the smallest average deviation between predicted and actual values. It also has the highest R^2 value, suggesting that it can explain most of the variability in the data. GPR, on the other hand, has the lowest MAPE, implying that it has the smallest percentage error in predicting the feed force. Linear regression (LR), principal component regression (PCR), and partial least square regression (PLSR) have comparable performance in terms of RMSE, MAE, R^2, and MAPE. They are outperformed by DT and GPR but perform better than support vector regression (SVR), neural network (NN), and ensemble learning-based regression (EM). SVR and NN have the highest RMSE and MAE, indicating that they have the largest average deviation between predicted and actual values. They also have the lowest R^2 values, suggesting that they cannot explain much of the variability in the data.

The results demonstrate that nonlinear models such as DT and GPR can capture the complex relationship between cutting parameters and machining force components better than linear models such as LR, PCR, and PLSR. Additionally, the relatively poor performance of SVR and NN may be attributed to the limited size of the dataset and the high autocorrelation in the HRC variable. Overall, the results suggest that GPR and DT are the most appropriate models for predicting feed force in the hard turning process of AISI 52100 bearing steel.

(b) Radial force prediction

We also predicted the radial force using the eight models. Figure 8 shows the predictions of radial force from the considered models based on testing data. From the plot, we can observe that all models can predict the trend of the radial force fairly well. However, there are some differences in the accuracy of the models in terms of the magnitude of the force. The DTR and GPR models seem to have the best performance. The NN, LR, and SVR models appear to perform relatively poorly, with larger deviations from the actual data.

Figure 9 presents the boxplots of the prediction errors from each model based on the fivefold cross-validation. The boxplots show that the decision tree regression (DTR) model has the lowest median of the prediction errors and the smallest interquartile range, indicating high accuracy and consistency. The Gaussian process regression (GPR) model also performs well, with a small interquartile range and a low median error. The other models, including linear regression (LR), principal component regression (PCR), partial least squares regression (PLSR), support vector regression (SVR), neural network

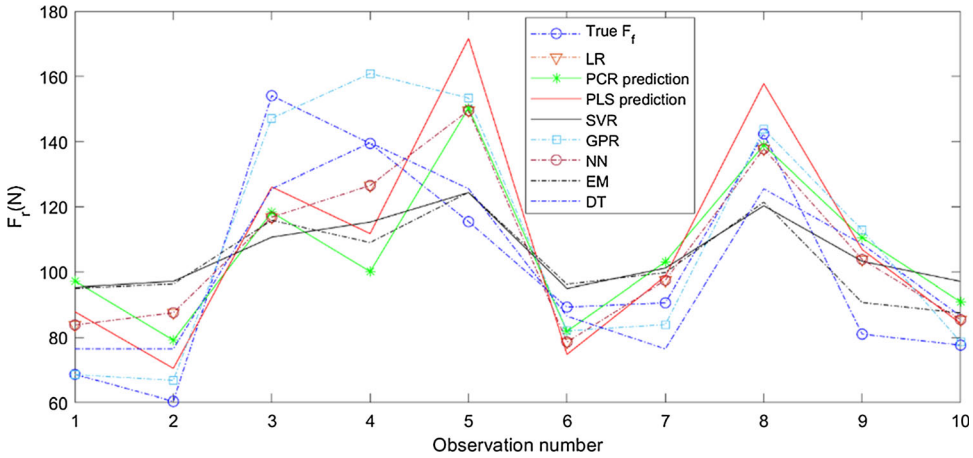

Fig. 8 Measured vs. predicted radial force using the eight models based on testing data

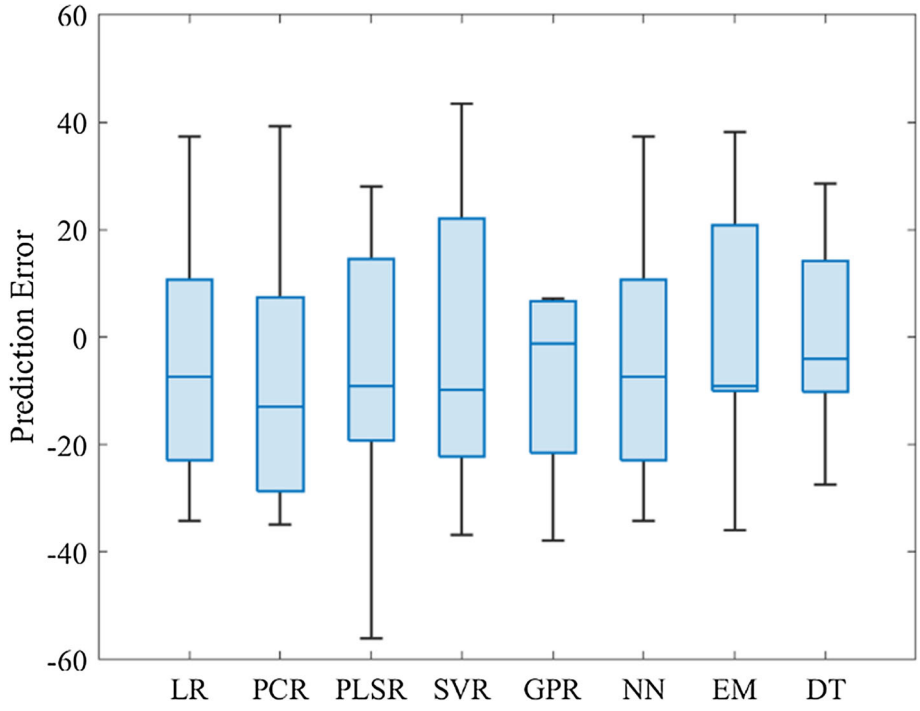

Fig. 9 Boxplots of prediction errors of the investigated models based on testing data

(NN), and ensemble learning-based regression (EM) models, show larger interquartile ranges and higher median errors than DTR and GPR models.

Based on the evaluation metrics in Table 5, the results show that Gaussian process regression (GPR) outperforms all other models regarding RMSE, MAE, R^2, and MAPE. This indicates that GPR is the most accurate model for predicting the radial force based on the given dataset. Decision tree regression (DTR) also performed well, with the second-lowest RMSE, MAE, and MAPE and the highest R^2. This suggests that DTR is a suitable alternative to GPR, especially since DTR is a simpler model and easier to interpret. On the other hand, support vector regression (SVR) and neural network (NN) showed poor performance, with the highest RMSE and MAE values and the lowest R^2. Overall, the results indicate that GPR and DTR are promising models for predicting the radial force in the given dataset, while SVR and NN may not be suitable for this task.

Table 5 Evaluation metrics over the testing sets for the eight models when predicting radial force

Method	RMSE	MAE	R^2	MAPE
LR	21.10	17.94	0.58	16.92
PCR	25.45	22.35	0.38	21.08
PLSR	25.29	21.17	0.42	18.53
SVR	24.73	22.00	0.41	20.96
GPR	17.63	12.11	0.75	9.98
NN	21.10	17.94	0.58	16.92
EM	22.84	19.67	0.49	18.89
DT	16.01	13.29	0.75	13.29

(c) Tangential force prediction

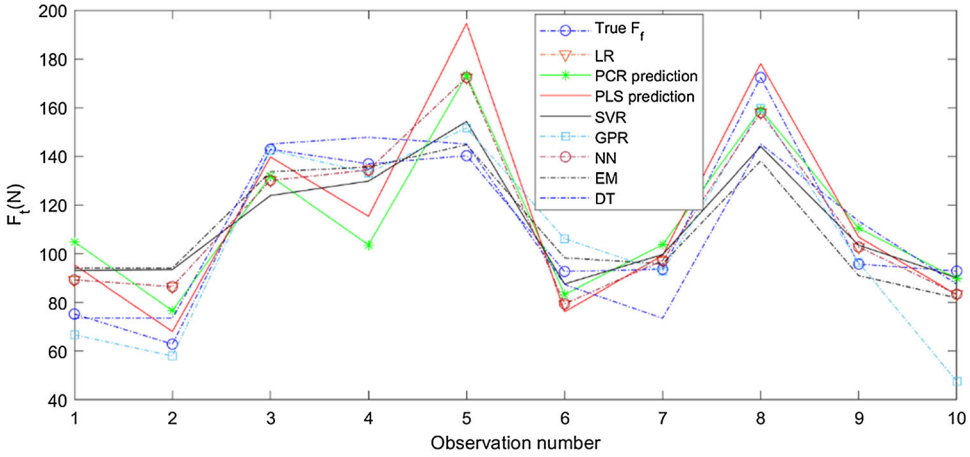

Fig. 10 Measured vs. predicted tangential force using the eight models based on testing data

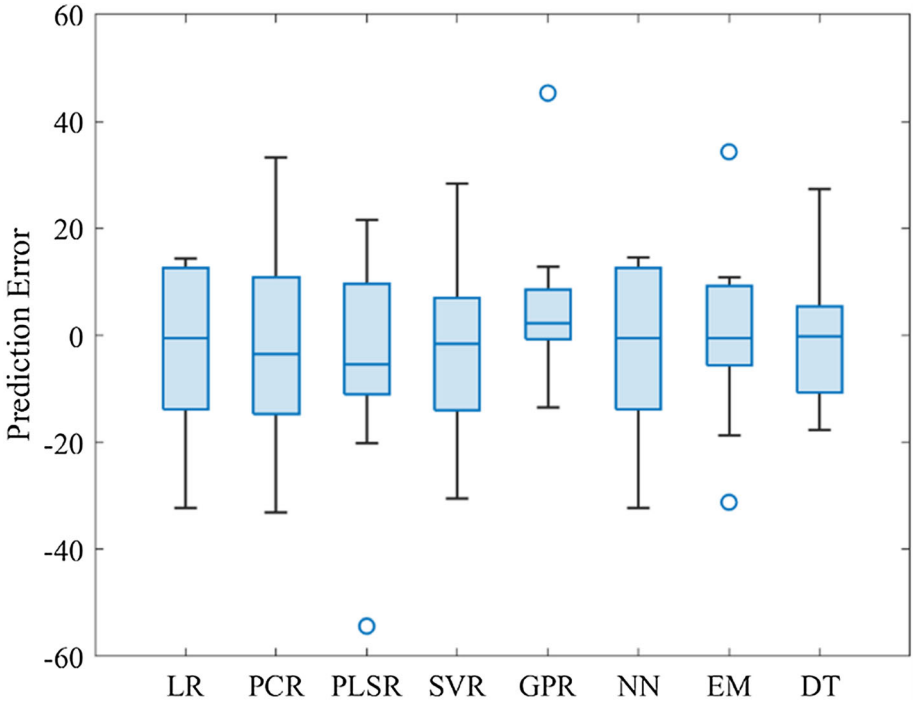

Fig. 11 Boxplots of prediction errors of the investigated models based on testing data

Table 6 Evaluation metrics over the test sets for the eight models when predicting tangential force

Method	RMSE	MAE	R^2	MAPE
LR	15.79	13.26	0.78	12.08
PCR	19.95	17.11	0.65	15.18
PLSR	21.00	15.30	0.63	13.02
SVR	16.71	13.86	0.75	12.40
GPR	16.24	10.20	0.79	14.95
NN	15.78	13.26	0.78	12.08
EM	16.70	12.29	0.75	11.57
DT	13.36	10.61	0.84	10.31

Finally, we assess the performance of the considered models in predicting tangential force. Figure 10 shows the measured and predicted tangential force using the considered models based on testing data. Based on the prediction plots (Fig. 10), we can see that all models are able to capture the general trend of the tangential force. However, some models appear to have more variability in their predictions than others, as seen in the wider range of the prediction intervals (Fig. 11). Table 6 shows the evaluation results of the investigated methods for predicting tangential force. The results suggest that GPR and DT have the lowest RMSE and MAE, indicating that they are more accurate in predicting tangential force compared to the other methods. Additionally, GPR has the highest $R2$ value, indicating a better fit of the model to the data, and the lowest MAPE value, indicating that the predictions are closer to the true values. These results suggest that GPR is the most effective method for predicting tangential force among the methods evaluated.

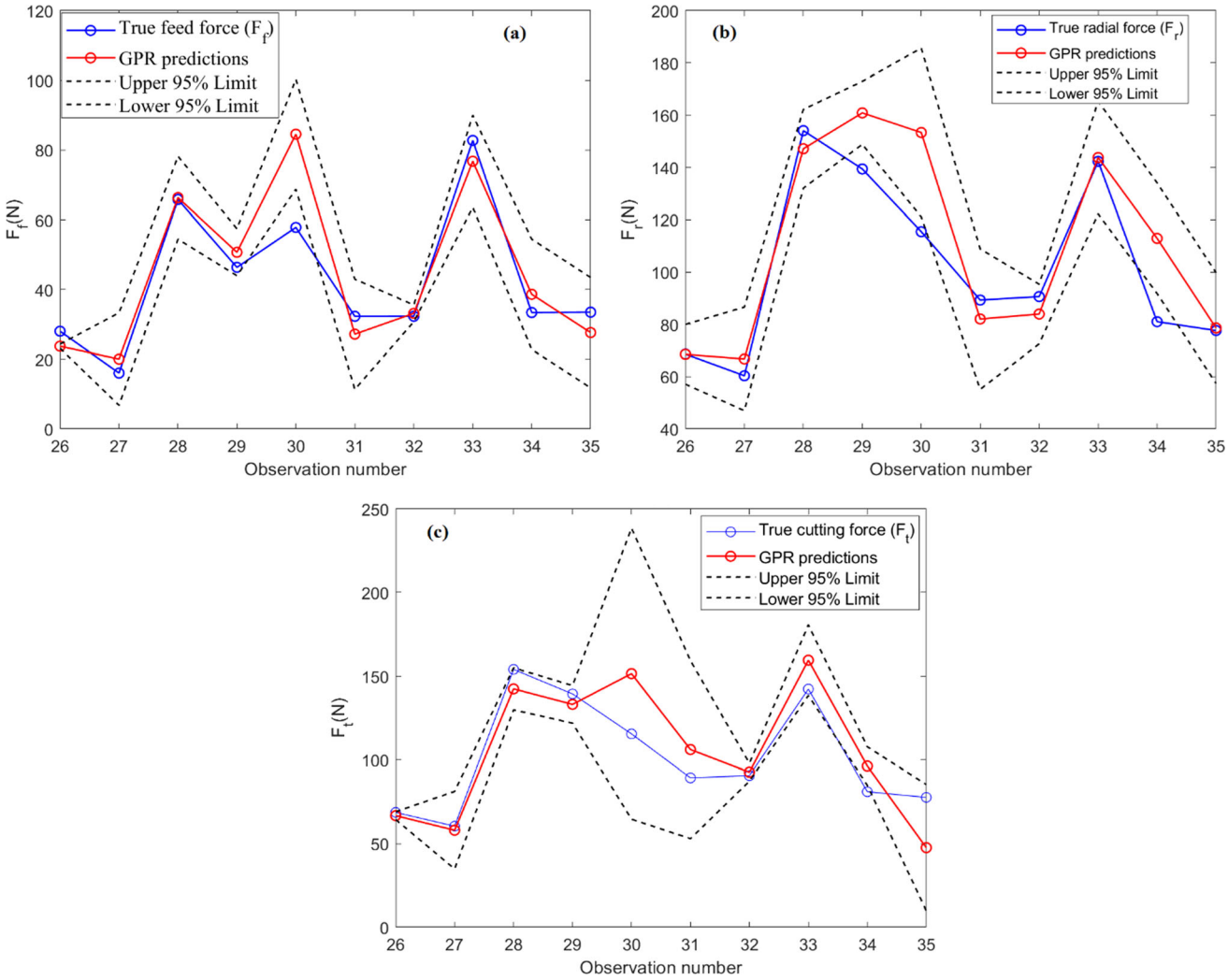

Fig. 12 GPR prediction with 95% confident interval: (a) feed force, (b) radial force, and (c) tangential force

Table 7 Metrics evaluation averaged across each approach

Method	RMSE	MAE	R^2	MAPE
LR	15.65	13.07	0.70	15.65
PCR	18.68	16.12	0.58	18.57
PLSR	18.97	14.98	0.59	16.70
SVR	20.10	15.16	0.44	16.32
GPR	14.44	9.53	0.77	13.08
NN	18.23	13.59	0.53	15.05
EM	16.56	13.19	0.66	15.74
DT	12.72	10.14	0.80	12.79

Figure 12(a-c) displays the prediction results of the GPR model of the feed, radial, and tangential forces based on testing data. The predicted values are very close to the observed values inside the 95% confidence interval. This level of accuracy is not achievable with the other machine learning models investigated, such as SVR, NN, and DT, making the GPR model very useful for predicting machining forces. This means that the GPR model can accurately predict the cutting forces, and its predictions are reliable. It makes the GPR model very helpful in providing reliable predictions and assessing the level of uncertainty associated with the predictions. Overall, the GPR model's ability to provide accurate and reliable predictions, along with the assessment of uncertainty, can be beneficial in improving the quality and efficiency of machining processes in the manufacturing industry.

In summary, the performance of eight models was evaluated, and their averaged metrics were tabulated and sorted by MAPE in Table 7. The DT model had the highest accuracy overall, followed by the GPR model, according to the barplot of MAPE values shown in Fig. 13. GPR provides uncertainty information about the predictions, while DT only provides point estimates. GPR models the underlying function as a distribution over functions, whereas DT models the data by recursively partitioning the feature space. Depending on the specific requirements and goals of a given application, one may choose to use either GPR or DT. DT may be preferred for accurate point predictions with interpretable models, while GPR may be a better choice for uncertainty information or modeling complex nonlinear relationships.

3.3 Feature Importance Identification

This study investigated the important features influencing the prediction of cutting forces (tangential, radial, and feed

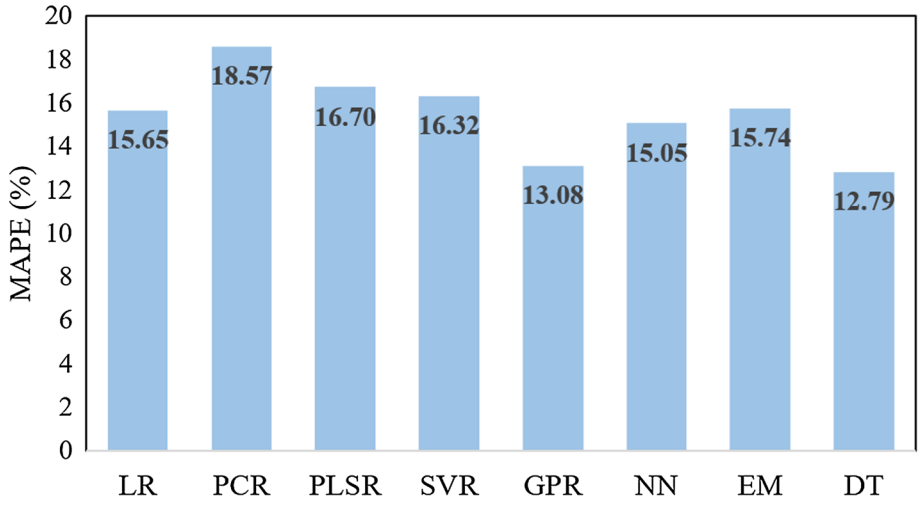

Fig. 13 A bar chart depicting the average MAPE values for each approach

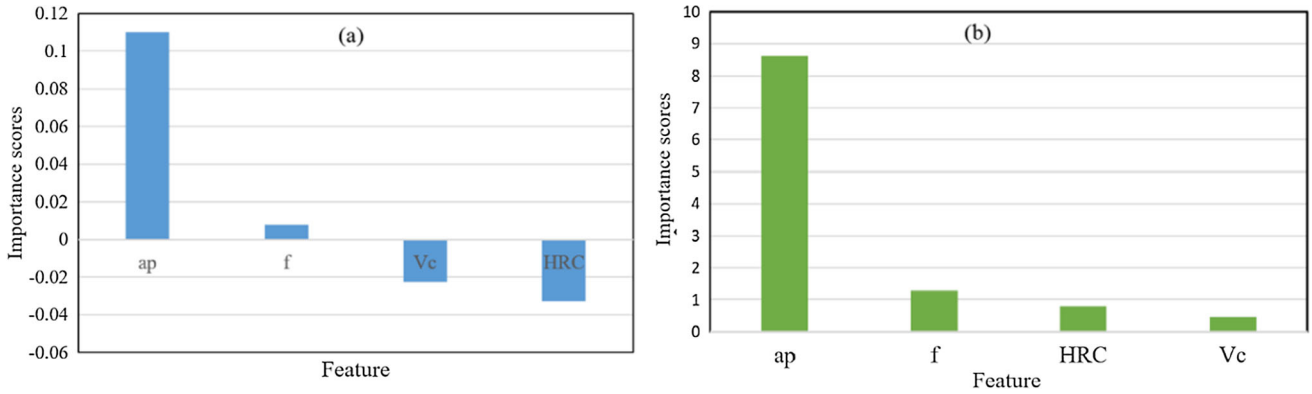

Fig. 14 Feature importance identification based on (a) RReliefF and (b) F test for feed force prediction

forces) in hard turning processes. To this end, two feature selection algorithms, namely RReliefF and F test, were applied.

- F test algorithm: This algorithm ranks the features based on their correlation with the response variable. It calculates the F-statistic and p value for each feature and selects the ones with the lowest p values. A higher F-value indicates a more important feature. The F-test algorithm is widely used in feature selection due to its simplicity and effectiveness. However, it should be noted that F-test algorithm assumes that the relationship between the features and the output is linear and may not work well for nonlinear relationships.
- Regressional Relief-F (RReliefF): RReliefF is a feature selection algorithm that utilizes the ReliefF algorithm to select the most important features. It randomly samples the data and determines the feature weights based on the relevance and redundancy between features (Ref 48). The algorithm then iteratively updates the weights based on the importance of the features in predicting the target variable. The features with the highest weights are considered the most important for prediction. The advantage of RReliefF is its ability to handle noisy data and identify the most relevant and informative features. It also works well for high-dimensional data and can handle both discrete and continuous features. This study used RReliefF to select important features for predicting cutting forces in hard turning processes.

Figure 14(a-b) shows the feature importance scores obtained by the RReliefF and F test algorithms for feed force prediction. Both algorithms rank a_p (depth of cut) as the most important feature for predicting feed force. For both algorithms, f (feed) has a low importance score. However, the importance rankings for the other two features, HRC and V_c, differ between the two algorithms. HRC is ranked higher by F test, while V_c is ranked higher by RReliefF. This highlights the importance of comparing results obtained by different feature selection algorithms, as they may prioritize different features depending on the underlying statistical assumptions and computational methods. In short, the results suggest that depth of cut is the most important feature for predicting feed force in hard turning processes, while feed has a lesser impact. However, HRC and V_c have less importance in predicting feed force.

Similarly, we applied the RReliefF and F test algorithms to identify the important parameters affecting the prediction of radial force (Fig. 15a-b). The results suggest that the feed plays a more significant role in predicting radial force compared to the other input parameters. Feed (f) may have the highest impact on the prediction of radial force because it is directly related to the amount of material being removed per unit of time, affecting the magnitude and direction of the radial force.

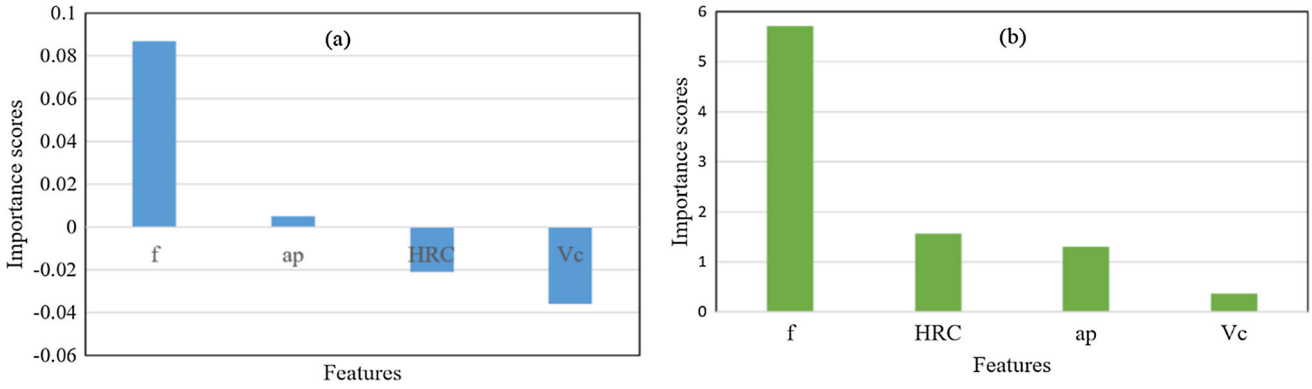

Fig. 15 Feature importance identification based on (a) RReliefF and (b) F test for radial force prediction

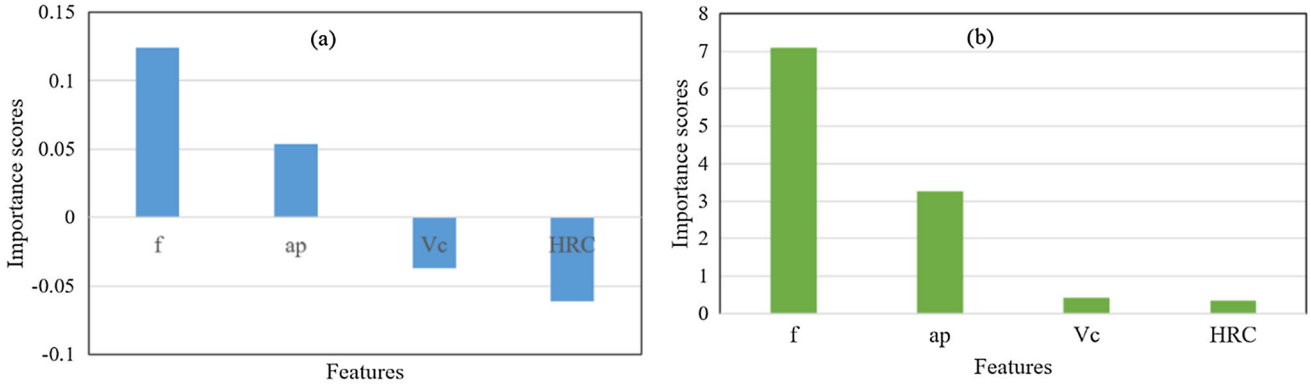

Fig. 16 Feature importance identification based on (a) RReliefF and (b) F test for tangential force prediction

Higher feed would lead to larger amounts of material being removed, resulting in larger radial forces. In addition, the feed can also affect the temperature of the cutting zone, which can influence the material's properties, and, ultimately, the magnitude of the radial force.

Finally, we applied the RReliefF and F test algorithms to identify the important parameters affecting the prediction of tangential force (Fig. 16a-b). Based on the F test scores, the most important feature for predicting tangential force is f (feed), with a score of 7.096, followed by a_p (depth of cut), with a score of 3.2641. The least important features are V_c (cutting speed) and HRC (hardness of the workpiece), with scores of 0.4193 and 0.3377, respectively. On the other hand, based on the RReliefF scores, the most important feature for predicting tangential force is f (feed), with a score of 0.1239, followed by a_p (depth of cut), with a score of 0.0536. The least important features are V_c (cutting speed) and HRC (hardness of the workpiece), with scores of $-$ 0.0371 and $-$ 0.061, respectively. Based on the F test and RReliefF scores, it can be concluded that the feed (f) and depth of cut (a_p) are the two most important features in predicting tangential force. Both algorithms have ranked f and a_p as the top two features, indicating their high impact on tangential force prediction. Indeed, feed and depth of cut are critical parameters in machining processes that can significantly affect tangential force. A higher feed or depth of cut typically results in higher tangential, as more material is being removed per unit of time.

In summary, these findings suggest that feed and depth of cut should be carefully controlled and optimized to improve the prediction and control of cutting forces in hard turning processes. The importance of surface hardness may also indicate the need for proper material selection and heat treatment. Cutting speed, while still an important factor in the process, may have a more limited impact on predicting cutting forces compared to feed and depth of cut. Overall, this study highlights the usefulness of feature selection algorithms in identifying the most important features for predicting cutting forces and may help optimize the hard turning process.

4. Conclusion

This study explored the feasibility of machine learning models in predicting the cutting forces during hard turning of AISI 52100 bearing steel using a CBN cutting tool. The performance of eight machine learning models was evaluated based on four statistical metrics. The results showed that decision tree and Gaussian process regression outperformed the other models, with average mean absolute errors of 9.53 and 10.14, respectively. The GPR model also incorporated modeling uncertainty into the predictions, which can be useful in

optimizing the cutting process and reducing tool wear. Using RReliefF and F test algorithms, the most important variables in predicting the cutting forces were found to be workpiece hardness, cutting speed, feed, and depth of cut. Identifying these variables can help operators optimize the cutting parameters to minimize tool wear and improve productivity and can also aid engineers and researchers in better understanding the physics of the machining process for more efficient tool design and process development. Overall, the results indicate that machine learning models can be a valuable tool for predicting cutting forces in hard turning processes, which can help improve process control, reduce tool wear, and enhance productivity.

The satisfactory results obtained in this study demonstrate the potential of machine learning models in predicting cutting forces during hard turning processes. However, future studies can develop more accurate and comprehensive models by addressing a few limitations. Firstly, the experimental dataset used was relatively small, and future studies could benefit from using larger datasets. Additionally, the study only considered three cutting force components, and other force components could be included to provide a more comprehensive analysis of the cutting forces. Finally, the study focused only on predicting cutting forces in hard turning processes, and other process variables, such as surface roughness, tool wear, and tool life, could be studied to provide a more complete understanding of the hard turning process.

Future work can explore the effect of using different cutting tool materials and workpiece materials on the accuracy of cutting force prediction models. Additionally, further research can be conducted to optimize the cutting parameters based on the predicted cutting forces to improve surface quality and reduce tool wear, the generated heat during machining, and cutting time to extend tool life.

References

1. S.K.S.R. Schmid, Manufacturing Engineering and Technology. *J. Mater. Process. Technol.* (2013)
2. S. Makhfi, K. Haddouche, A. Bourdim, and M. Habak, Modeling of Machining Force in Hard Turning Process, *Mech. Kauno Technol. Univ.*, 2018, **24**(3), p 367–375
3. M.W. Azizi, O. Keblouti, L. Boulanouar, and M.A. Yallese, Design Optimization in Hard Turning of E19 Alloy Steel by Analysing Surface Roughness, Tool Vibration and Productivity, *Struct. Eng. Mech.*, 2020, **73**(5), p 501–513
4. S. Roy, R. Kumar, A.K. Sahoo, A. Pandey, and A. Panda, Investigation on Hard Turning Temperature under a Novel Pulsating MQL Environment: An Experimental and Modelling Approach, *Mech. Ind.*, 2020, **21**(6), p 605
5. A. Chavan and V. Sargade, Surface Integrity of AISI 52100 Steel during Hard Turning in Different Near-Dry Environments, *Adv. Mater. Sci. Eng.*, 2020, **2020**, p 1
6. F.K. Branco, S. Delijaicov, É.C. Bordinassi, and R. Bortolussi, Surface Integrity Analisys in the Hard Turning of Cemented Steel AISI 4317, Mater. Res., 2018, **21**(5)
7. P. Kumar, S.R. Chauhan, C.I. Pruncu, M.K. Gupta, D.Y. Pimenov, M. Mia, and H.S. Gill, Influence of Different Grades of CBN Inserts on Cutting Force and Surface Roughness of AISI H13 Die Tool Steel during Hard Turning Operation, Materials (Basel)., MDPI AG, 2019, **12**(1)
8. P. Umamaheswarrao, D. Rangaraju, K.N.S. Suman, and B. Ravisankar, Machining Force Comparison for Surface Defect Hard Turning and Conventional Hard Turning of AISI 52100 Steel, *INCAS Bull.*, 2021, **13**(3), p 205–214
9. C. Cappellini and A. Abeni, Development and Implementation of Crater and Flank Tool Wear Model for Hard Turning Simulations, *Int. J. Adv. Manuf. Technol.*, 2022, **120**(3–4), p 2055
10. M. Marconi and R. Menghi, A Sustainable Manufacturing Tool for the Analysis and Management of Resource Consumption within Production Processes, *Int. J. Interact. Des. Manuf.*, 2021, **15**(1), p 65
11. W. Cai and K. Hung Lai, Sustainability Assessment of Mechanical Manufacturing Systems in the Industrial Sector, *Renew. Sustain. Energy Rev.*, 2021, **135**, p 110169
12. M. Jamil, A.M. Khan, N. He, L. Li, A. Iqbal, and M. Mia, Evaluation of Machinability and Economic Performance in Cryogenic-Assisted Hard Turning of α-β Titanium: A Step towards Sustainable Manufacturing, *Mach. Sci. Technol.*, 2019, **23**(6), p 1022
13. R. Nur, N.M. Yusof, I. Sudin, F.M. Nor, and D. Kurniawan, Determination of Energy Consumption during Turning of Hardened Stainless Steel Using Resultant Cutting Force, *Metals (Basel)*, 2021, **11**(4), p 565
14. A. Sahinoglu and E. Ulas, An Investigation of Cutting Parameters Effect on Sound Level, Surface Roughness, and Power Consumption during Machining of Hardened AISI 4140, *Mech. Ind.*, 2020, **21**(5), p 523
15. Y. Yu, X. Wu, and Q. Qian, Better Utilization of Materials' Compositions for Predicting Their Properties: Material Composition Visualization Network, *Eng. Appl. Artif. Intell.*, 2023, **117**, p 105539. https://doi.org/10.1016/j.engappai.2022.105539
16. A. Dorbane, F. Harrou, and Y. Sun, Exploring Deep Learning Methods to Forecast Mechanical Behavior of FSW Aluminum Sheets, *J. Mater. Eng. Perform.*, 2022 https://doi.org/10.1007/s11665-022-07376-1
17. A. Dorbane, F. Harrou, and Y. Sun, "A Tree-Driven Ensemble Learning Approach to Predict FS Welded Al-6061-T6 Material Behavior," *2022 7th International Conference on Frontiers of Signal Processing (ICFSP)*, IEEE, 2022, p 184–188, doi:https://doi.org/10.1109/ICFSP55781.2022.9924883
18. K. Guo, Y. Zhenze, C.-H. Yu, and M. Buehler, Artificial Intelligence and Machine Learning in Design of Mechanical Materials, *Mater. Horiz.*, 2021, **8**, p 1153
19. M. Fernandes, J.M. Corchado and G. Marreiros, Machine Learning Techniques Applied to Mechanical Fault Diagnosis and Fault Prognosis in the Context of Real Industrial Manufacturing Use-Cases: A Systematic Literature Review, *Appl. Intell.*, 2022, **52**(12), p 14246–14280. https://doi.org/10.1007/s10489-022-03344-3
20. K. Singh and I.A. Sultan, A Computer-Aided Sustainable Modelling and Optimization Analysis of Cnc Milling and Turning Processes, *J. Manuf. Mater. Process.*, 2018, **2**(4), p 65
21. D. Cica, B. Sredanovic, and S. Tesic, Predictive Modeling of Turning Operations under Different Cooling / Lubricating Conditions for Sustainable Manufacturing with Machine Learning Techniques, (2020)
22. A. Das, S.R. Das, J.P. Panda, A. Dey, K.K. Gajrani, N. Somani, and N. Gupta, Machine Learning Based Modelling and Optimization in Hard Turning of AISI D6 Steel with Newly Developed AlTiSiN Coated Carbide Tool, 2022, doi:https://doi.org/10.48550/arxiv.2202.00596
23. C. Du, C.L. Ho, and J. Kaminski, Prediction of Product Roughness, Profile, and Roundness Using Machine Learning Techniques for a Hard Turning Process, *Adv. Manuf.*, 2021, **9**(2), p 206–215. https://doi.org/10.1007/s40436-021-00345-2
24. S. Makhfi, M. Habak, R. Velasco, K. Haddouche, and P. Vantomme, Prediction of Cutting Forces Using ANNs Approach in Hard Turning of AISI 52100 Steel, *AIP Conf. Proc.*, American Institute of Physics, 2011, **1353**(1), p 669-674, doi:https://doi.org/10.1063/1.3589592
25. A. Panda, A.K. Sahoo, I. Panigrahi, and A.K. Rout, Investigating Machinability in Hard Turning of AISI 52100 Bearing Steel Through Performance Measurement: QR, ANN and GRA Study, *Int. J. Automot. Mech. Eng.*, 2018, **15**(1), p 4935–4961. https://doi.org/10.15282/ijame.15.1.2018.5.0384
26. A.K. Sahoo, A.K. Rout, and D.K. Das, Response Surface and Artificial Neural Network Prediction Model and Optimization for Surface Roughness in Machining, *Int. J. Ind. Eng. Comput.*, 2015, **6**(2), p 229–240
27. R. Kumar, A.K. Sahoo, P.C. Mishra, R.K. Das, and M. Ukamanal, Experimental Investigation on Hard Turning Using Mixed Ceramic Insert under Accelerated Cooling Environment, *Int. J. Ind. Eng. Comput.*, 2018, **9**(4), p 509–522

28. A. Panda, A.K. Sahoo, and A.K. Rout, Investigations on Surface Quality Characteristics with Multi-Response Parametric Optimization and Correlations, *Alexandria Eng. J.*, 2016, **55**(2), p 1625–1633
29. A.K. Sahoo, K. Orra, and B.C. Routra, Application of Response Surface Methodology on Investigating Flank Wear in Machining Hardened Steel Using PVD TiN Coated Mixed Ceramic Insert, *Int. J. Ind. Eng. Comput.*, 2013, **4**(4), p 469–478
30. R.K. Das, A.K. Sahoo, P.C. Mishra, R. Kumar, and A. Panda, Comparative Machinability Performance of Heat Treated 4340 Steel under Dry and Minimum Quantity Lubrication Surroundings, *Procedia Manuf.*, 2018, **20**, p 377–385
31. A. Panda, A.K. Sahoo, R. Kumar, and R.K. Das, A Review on Machinability Aspects for AISI 52100 Bearing Steel, *Mater. Today Proc.*, 2020, **23**, p 617–621
32. I. Urresti, I. Llanos, J. Zurbitu, and O. Zelaieta, Tool Wear Modelling of Cryogenic-Assisted Hard Turning of AISI 52100. *Procedia CIRP*, (2021)
33. P. Umamaheswarrao, D. Ranga Raju, K.N.S. Suman, and B. Ravi Sankar, Hybrid Optimal Scheme for Minimizing Machining Force and Surface Roughness in Hard Turning of AISI 52100 Steel, *Int J Eng Sci Technol.*, 2019, **11**(3), p 19–29
34. A. Anand, A.K. Behera, and S.R. Das, An Overview on Economic Machining of Hardened Steels by Hard Turning and Its Process Variables, *Manuf. Rev.*, 2019, **6**, p 4
35. S. Makhfi, Modélisation et Simulation Du Comportement Thermomécanique de l'usinage à Grande Vitesse. (2018)
36. I.E. Frank and J.H. Friedman, A Statistical View of Some Chemometrics Regression Tools, *Technometrics*, [Taylor & Francis, Ltd., American Statistical Association, American Society for Quality], 1993, **35**(2), p 109–135, doi:https://doi.org/10.2307/1269656
37. B. Bouyeddou, F. Harrou, A. Saidi, and Y. Sun, An Effective Wind Power Prediction Using Latent Regression Models, in *2021 International Conference on ICT for Smart Society (ICISS)*, 2021, p 1–6
38. P. Geladi and B.R. Kowalski, Partial Least-Squares Regression: A Tutorial, *Anal. Chim. Acta*, 1986, **185**, p 1–17. https://doi.org/10.1016/0003-2670(86)80028-9
39. W. Loh, Classification and Regression Trees, *Wiley Interdiscip. Rev. data Min. Knowl. Discov.*, 2011, **1**(1), p 14–23
40. W. Hong, Y. Dong, L.-Y. Chen, and S.-Y. Wei, SVR with Hybrid Chaotic Genetic Algorithms for Tourism Demand Forecasting, *Appl. Soft Comput.*, 2011, **11**, p 1881–1890
41. A.J. Smola and B. Schölkopf, A Tutorial on Support Vector Regression, *Stat. Comput.*, 2004, **14**(3), p 199–222. https://doi.org/10.1023/B:STCO.0000035301.49549.88
42. J. Lee, W. Wang, F. Harrou, and Y. Sun, Reliable Solar Irradiance Prediction Using Ensemble Learning-Based Models: A Comparative Study, *Energy Convers. Manag.*, 2020, **208**, p 112582
43. J. Lee, W. Wang, F. Harrou, and Y. Sun, Wind Power Prediction Using Ensemble Learning-Based Models N3—https://doi.org/10.1109/ACCESS.2020.2983234. *IEEE Access*, 2020, http://hdl.handle.net/10754/662323
44. F. Harrou, A. Saidi, Y. Sun, and S. Khadraoui, "Monitoring of Photovoltaic Systems Using Improved Kernel-Based Learning Schemes N3—https://doi.org/10.1109/JPHOTOV.2021.3057169," *IEEE Journal of Photovoltaics*, 2021, http://hdl.handle.net/10754/667699
45. C.E. Rasmussen and C.K.I. Williams, Gaussian Processes for Machine Learning, *Gaussian Processes for Machine Learning*, (Cambridge, MA, USA), The MIT Press, 2006, doi:https://doi.org/10.7551/mitpress/3206.001.0001
46. L. Tang, L. Yu, S. Wang, J. Li, and S. Wang, A Novel Hybrid Ensemble Learning Paradigm for Nuclear Energy Consumption Forecasting, *Appl. Energy*, 2012, **93**, p 432
47. Q. Pan, F. Harrou, and Y. Sun, A Comparison of Machine Learning Methods for Ozone Pollution Prediction, *J. Big Data*, 2023, **10**(1), p 1–31. https://doi.org/10.1186/S40537-023-00748-X
48. M. Robnik-Šikonja and I. Kononenko, Theoretical and Empirical Analysis of ReliefF and RReliefF, *Mach. Learn.*, 2003, **53**(1), p 23–69. https://doi.org/10.1023/A:1025667309714